冯绪杨，伍伟文，朱慧杰，等. 一种锥束 CT 动态 Bowtie 的蒙特卡罗模拟研究（英）[J]. CT 理论与应用研究，2018，27(3)：315-327. doi:10.15953/j.1004-4140.2018.27.03.04.
Feng XY, Wu WW, Zhu HJ, et al. Monte Carlo simulation for a dynamic bowtie filter with cone-beam CT[J]. CT Theory and Applications, 2018, 27(3): 315-327. doi:10.15953/j.1004-4140.2018.27.03.04.

Monte Carlo Simulation for a Dynamic Bowtie Filter with Cone-beam CT

FENG Xu-yang[1], WU Wei-wen[2], ZHU Hui-jie[1], YU Hai-jun[1], LIU Feng-lin[1,2]✉

1. College of Mechanical Engineering, Chongqing University, Chongqing 400044, China
2. ICT Research Center, Chongqing University, Chongqing 400044, China

Abstract: A pre-patient attenuator (“Bowtie filter” or "Bowtie") in X-ray computed tomography (CT) is used for reducing the radiation dose to patients and helping meet the detector dynamic range, and it also affects the CT image quality. Because a traditional static Bowtie filter is not optimal for modulating X-ray, we recently proposed a dynamic Bowtie filter for cone-beam CT, which could modulate X-ray more effectively. In this paper, we design and study the dynamic Bowtie using Monte Carlo simulation. First, we establish a simulation frame, which contains a target phantom and a polychromatic source generated by a reflection target. Next, a design phantom is employed to help design the dynamic Bowtie for the target phantom. Finally, we obtain two phantom projections from two modes of filter: no Bowtie and the dynamic Bowtie. The results demonstrate that, under the action of the designed dynamic Bowtie, the X-ray dynamic range on detectors is highly compressed for the design phantom and the target phantom, which means that our methodology facilitate to uniform the photon flux. Moreover, with the uniformed photon flux, the radiation exposure suffered by tested objects reduces and the reconstructed image quality is improved.

Keywords: computed tomography; cone-beam; dynamic Bowtie; Monte Carlo simulation

doi:10.15953/j.1004-4140.2018.27.03.04 **CLC number:** O 242；TP 391 **Document code:** A

To detect the finer interior structure within patients, CT has been widely used in medical diagnosis. In the medical field, reducing the amount of X-ray radiation dose irradiated to the human body is also a public health problem, given the increasing risk of cancer[1-2]. To address such problems, a pre-patient attenuator, known as a static “Bowtie filter” was developed[3]. As the result of its special spatial shape, the less attenuating parts of the patient has a lower level of X-ray exposure. Meanwhile, the photon flux on the detector also becomes minimal and more consistent, which is beneficial to the detectors, having a narrow dynamic range[4]. Moreover, the X-ray scattering is also reduced by reducing X-ray intensity passing through less attenuating parts of the patient, and the Bowtie also blocks low-energy X-ray such that the beam-hardening effects may be reduced. Thus, the image quality can be improved with a Bowtie[5-6]. However, as a static Bowtie stays fixed as the gantry rotates, it cannot effectively modulate each incoming X-ray beam to balance the photon flux on the detector array. Therefore, to obtain the maximum image quality at the minimum cost of radiation dose, dynamic Bowtie devices, whose shapes or attenuating materials can be dynamically adjusted, have been explored. To this end, several dynamic Bowtie devices have been reported[7].

Received date: 2018-03-22.
Foundation item: The National Natural Science Foundation of China (61471070); The National Instrumentation Program of China (2013YQ030629).

Two sophisticated dynamic Bowtie devices have been extensively studied. The first of them is the piecewise-linear dynamic Bowtie filter, which is made up of movable triangular wedges in the axial direction and can form different cross-sectional shapes that is corresponding to a specific patient[8]. By solving the optimization problems of minimizing the mean and peak variance subjected to a fixed-dose limit, the perfect profiles, minimizing the dynamic range, can be formed[9]. The second of them is the digital beam attenuator, which can form cross-sectional shapes with respect to patients' shapes and sizes by moving a set of movable wedges over a set of stationary wedges. Thus, X-ray can be effectively modulated with the change of the projection angle by this dynamic Bowtie[10]. Moreover, Monte Carlo simulations have been employed to test the ability of the Bowties to compress the dynamic range and reduce the radiation dose. Simulation results show that both dynamic Bowtie filters can effectively compress the dynamic range and reduce the radiation dose. Especially, compared to non-Bowtie, dynamic Bowtie devices achieved substantial gains in noise uniformity and scatter reduction, which are instrumental in improving the image quality[11-12]. While the Bowtie devices are novel and promising, they are still constantly being researched and improved due to their complexities.

Recently, we proposed a dynamic Bowtie device, which can not only be applied to fan-beam scans but also adapted to the cone-beam/multi-slice CT[13]. This Bowtie device consists of a highly attenuating module (HB) filled in with heavy liquid and a weakly attenuating module (WB) that is immersed in the liquid of the HB. During the scanning process, the WB is rotated synchronously with the rotation of the patient to maintain a smooth photon flux. In the preliminary study, we theoretically confirmed that this Bowtie can compress the dynamic range by simple control and that it can be extended from the fan-beam scan to the cone-beam/multi-slice scan. Next, we proposed a method to design the surface shape of the HB in the case of a polychromatic source[14].

Monte Carlo simulation is a statistical technique using random sampling. In radiology, Monte Carlo simulation has been widely applied to the research on the radiation dose, X-ray scattering and image correction[15-19]. In terms of the complexity of dynamic Bowtie devices, Monte Carlo simulations should be implemented to evaluate their performance. Thus, research and development costs are also largely reduced. The Monte Carlo package, a General Monte Carlo N-Particle Transport Code (MCNP), appeared early and has been widely used in nuclear physics and radiology[20].

In this paper, MCNP is used to design the dynamic Bowtie in the case of polychromatic source. In the initial section, we review the proposed dynamic Bowtie and establish a simulation frame for an elliptical target phantom. In the next section, a design phantom is used to design the dynamic Bowtie for the target phantom and acquire relevant simulation data of two scan modes of filter: no Bowtie and the dynamic Bowtie. In the third section, we show the results of the dynamic Bowtie in the dynamic range, radiation dose and image quality. In the last section, we present this study's conclusions and discuss relevant issues.

1 Frame

In this section, we present a simple review of our proposed dynamic Bowtie and build a simulation frame, which includes model layout, a target phantom, a polychromatic X-ray source and the constituent materials of the dynamic Bowtie.

1.1 Review of The Dynamic Bowtie

The dynamic Bowtie consists of the HB and the WB. The HB targets a smooth photon flux along the detector array when no object is in the field of view (FOV), and the WB is a scaled-down version of the object. As shown in Fig.1(a), if only the HB located in the FOV, the HB, which is filled with high attenuation liquid, can make the detection intensity along the detector array consistent. Meanwhile, if an object is in the FOV, the detection intensity will be reduced. Fortunately, the WB immersed in the HB makes up for the reduction of the detection intensity,

which is caused by the setting of the object (Fig.1(b)). Furthermore, for similarity between the WB and the object, the longer the X-ray length passing through object, the more compensation the WB produces. Theoretically, if the object has a uniform attenuation coefficient, according to the similitude ratio between the WB and the object, the equivalent attenuation coefficients of the HB and WB can be determined to make the detection intensity along the detector array exactly uniform. As shown in Fig.1(c), when the object rotates, the WB rotates at the same speed such that these relations remain unchanged. So, the detection intensities along the detector array keep uniform throughout the scanning process. These relations also remain the same for 3D (Fig.2), which means that the dynamic range will be compressed as well as for 2D. Thus, the dynamic Bowtie can be extended from the fan-beam scan to the cone-beam scan. For simplicity, the fan-beam data is employed to confirm the performance of the dynamic Bowtie.

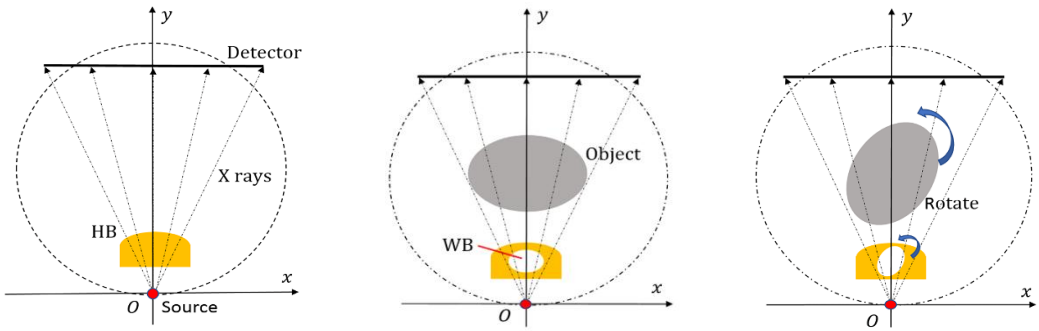

(a) Only the HB in the FOV　　(b) The WB immersed in the HB　　(c) The WB rotates with the object

Fig.1　Proposed dynamic Bowtie model

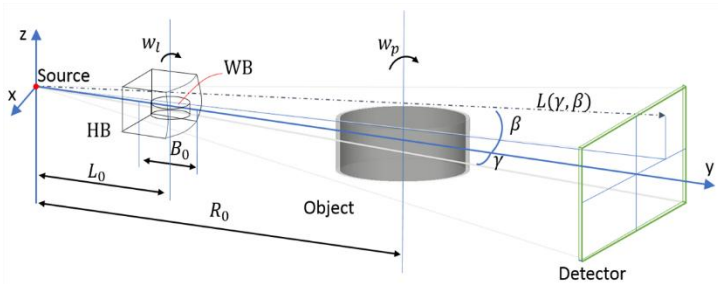

Fig.2　Dynamic Bowtie on basis of the 2D prior art

1.2　Simulation Frame

1.2.1　Polychromatic Source

In this section, we generated a reflecting target source. As shown in Fig.3(a), the electron beam with the energy of 160 keV strikes a tungsten target at a target angle 25^{o}, reflecting X-ray photons. A probe before the reflecting target tallies the relative photon flux of different energy segments.

To get MCNP simulation data, we need edit the input file and run it. The input file consists of some modules, which are defined by different cards. Based on the model in Fig.3(a), we edited the input file, which contains the necessary cells, the electronic source and the tally. In this simulation, the photon flux tallying card is used to tally the photons that are distributed between 0 keV and 160 keV and the result is shown in Fig.3(b). As is shown in Fig.3(b), the photons are mainly distributed in the low-energetic region, especially in the neighborhood of 10 keV and 60 keV.

The energy spectrum distribution from the reflecting target will be used to design and study the dynamic Bowtie.

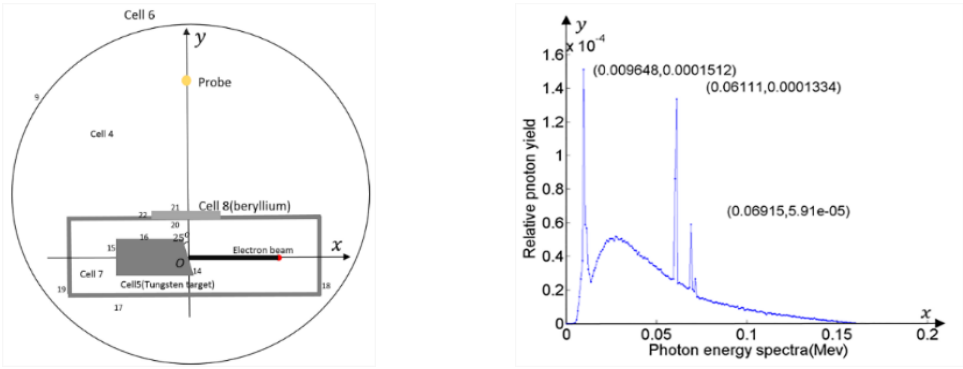

(a) The reflecting target model (b) The energy distribution of photons

Fig.3 Display of the polychromatic source

1.2.2 Target Phantom

In clinical applications, the proposed dynamic Bowtie targets a class of tested objects such as the human head, abdomen or chest. The type of tested object has common features in shape and constituent materials. In this study, an elliptical target phantom was employed to simulate such tested objects. We define the major-axis length of the target phantom as A_1, the semi-minor axis length of the target phantom as B_1 and the thickness of target phantom as T_p. The WB and the target phantom are similar in shape, and we assume the ratio between the two is *k*. So, the WB is a scale-down elliptical slice with the semi-major axis length kA_1, semi-minor axis length kB_1 and thickness kT_p. As shown in Fig.4, the target phantom is made of 5 different parts, which are respectively a ring slice, a circular slice, two empty oval slices and internal filling water and, in the case of monochromatic source of 130 keV，whose attenuation coefficients are respectively 0.507 cm^{-1}, 0.199 cm^{-1}, 0 cm^{-1} and 0.156 cm^{-1}.

1.2.3 Model Layout

As shown in Fig.5, the CT scan model with the dynamic Bowtie includes four parts: the source, the proposed dynamic Bowtie, the tested phantom and a detector array. For any ray angle γ in the FOV, the length L_γ of an X-ray passing through the HB and WB keeps a constant value B_0, which means that the detection intensity along the detector array keeps consistent without the tested phantom and WB. Next, we define the distances between the source and the center of the dynamic Bowtie and the center of the tested phantom as L_0 and R_0, respectively. To ensure that the ratios of all X-ray lengths through the WB and object are equal to *k*, L_0/R_0 should be *k*.

1.2.4 Materials of Dynamic Bowtie

First, the HB attenuating liquid was determined. Refer to the selection of attenuating liquid in the digital beam attenuator of the piston pipe[21], the $CeCl_3$ solution was considered as the HB attenuating liquid and we have tested its attenuating characteristics. As shown in Fig.6(a)，we built a simulation model, in which the reflecting target emits X-ray with intensity I_0 and a probe detects the attenuated X-ray with intensity I_b attenuated by a $CeCl_3$ solution module with length B_l. The model is used to implement two simulation experiments, one of which is aimed to test the relationship between the $CeCl_3$ solution concentration and the intensity I_b and the other of which is aimed to show the energy spectrum of the X-ray attenuated by $CeCl_3$ solution module with different lengths. In the first simulation experiment, the attenuation length B_l equals 8 cm and the result shows that I_b decreases sharply with the increase of $CeCl_3$ solution concentration (Fig.6(b)), which means that the $CeCl_3$ solution has heavy attenuation characteristic. In the second simulation

experiment, 30% $CeCl_3$ solution concentration is used to fill the module and the result shows that the energy spectrum of attenuated X-ray is more evenly distributed compared with that of X-ray emitted directly by the reflecting target (Fig.6(c)), which means that the $CeCl_3$ attenuation module can be used to get better X-ray. Therefore, the $CeCl_3$ solution with heavy attenuation characteristics is chosen as the attenuating liquid filling the HB.

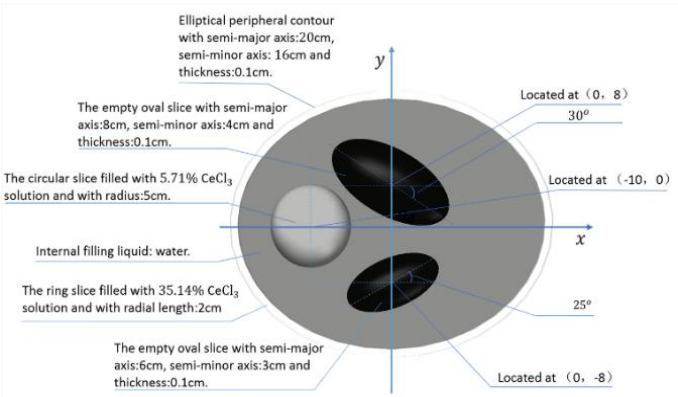

Fig.4　Display of the target phantom

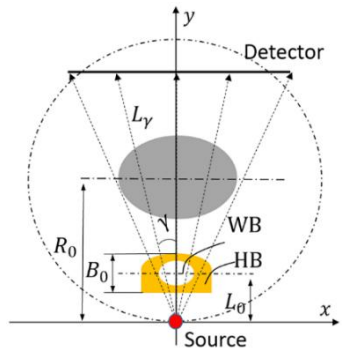

Fig.5　CT scan model with the proposed dynamic Bowtie

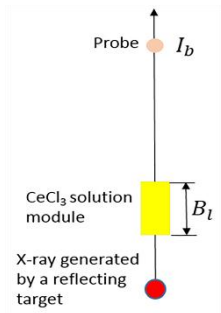

(a) The testing model

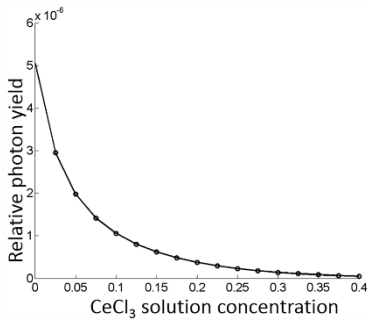

(b) The attenuation characteristics of $CeCl_3$ solution

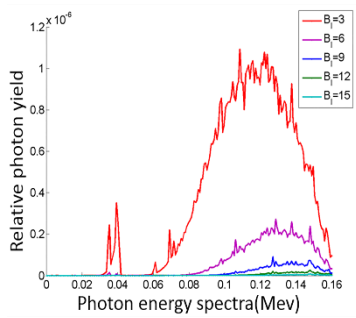

(c) The energy distribution of photons

Fig.6　The test of $CeCl_3$ solution

The WB has low attenuation characteristics and its attenuation coefficient can be approximated as the attenuation coefficient of air or 0. The aluminum is used as the HB container material, and C-552 air-equivalent plastic is used as the WB container material.

1.2.5　MCNP Simulation Frame

To summarize, we have obtained simulation parameters as shown in Table 1. As shown in Fig.7, the input files can be constructed based on the target phantom, the dynamic Bowtie, the energy spectrum from the reflecting target, corresponding data tally type, the running time and accuracy. In this simulation, considering the running time and accuracy, we choose the number of particles to be 1.0E+6.

In this paper, the circular scan data is required to verify the performance of the dynamic Bowtie and it can be acquired by 720 input files, which correspond to 720 projection angles. We define the projection angle as φ. First, we edit the input file at $\varphi = 0^o$. To get the data of the angle at $\varphi \neq 0^o$, a coordinate transformation card can be used to change the rotation angle of the simulation phantom and WB in other input files, which is done automatically by an auxiliary program.

Table 1 Simulation parameters

Parameter	Value
Scan radius (R_0)	57 cm
Distance of source to the proposed dynamic Bowtie (L_0)	19 cm
X-ray track's total length through HB and WB (B_0)	16 cm
Semi-major axis of the ellipse (A_1)	20 cm
Semi-minor axis of the ellipse (B_1)	18 cm
Thickness of the ellipse (T_p)	0.1 cm
Ratio of similitude (k)	1/3
Semi-major axis of WB (kA_1)	20/3 cm
Semi-minor axis of WB (kB_1)	16/3 cm
Thickness of WB (kT_p)	1/30 cm
Source to detector distance (SDD)	114 cm
Number of intermediate detector units (n)	672
Projection number in 360° (m)	720
Linear detector length	100 cm
HB container thickness	0.05 cm
WB container thickness	0.02 cm
WB attenuator	Air

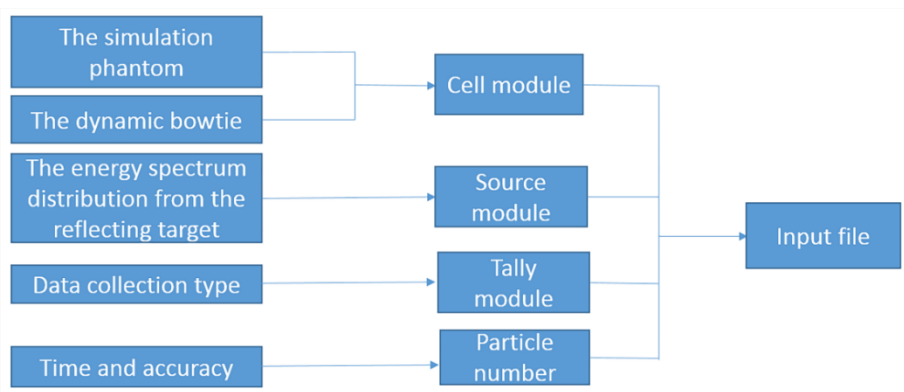

Fig.7 The structure of input file

2 Methodology

In this section, a design phantom is employed to design the dynamic Bowtie for the target phantom.

2.1 Design Phantom

In simulation, a design phantom also needs to be employed. On the one hand, a design phantom is employed to design the proposed dynamic Bowtie, making sure that the proposed dynamic Bowtie can effectively compress the dynamic range. On the other hand, this phantom can be used to clearly evaluate the contribution of the dynamic Bowtie in the radiation dose or image quality.

Although the internal attenuation coefficient of the object to be tested is not known, we can evaluate a constant attenuation value based on its basic constituent materials. Thus, a design phantom, which is made of uniform material with a constant attenuation value and has the same external shape as the target phantom can be easily made. In this paper, as water accounts for the largest proportion of the constituents of the target phantom, its attenuation value is evaluated as the constant attenuation value. Therefore, the design phantom consists of uniform water and has the same external shape as the target phantom.

2.2 $CeCl_3$ Solution Concentration

We define the equivalent attenuation coefficients of the design phantom, HB and WB as μ_p, μ_h and μ_w, respectively, and X-ray lengths through the design phantom and the WB as l_p and l_w, respectively, and total X-ray integral as P_t. Let I_0 be the intensity of source and I be the intensity of an X-ray after passing through the design phantom and Bowtie. We have

$$I = I_0 \exp(-p_t) = I_0 \exp\left(-\left(\int_{l_p} \mu_p \mathrm{d}l + \int_{B_o - l_w} \mu_h \mathrm{d}l + \int_{l_w} \mu_w \mathrm{d}l\right)\right) = I_0 \exp\left(-\left(B_o \mu_h + l_p\left(\mu_p + k\mu_w - k\mu_h\right)\right)\right) \tag{1}$$

If I is a constant value $I_0 \exp(-B_0\mu_h)$, we have

$$\mu_p + k\mu_w - k\mu_h = 0 \tag{2}$$

The above formula is not in respect to the ray angle γ and projection angle φ. Therefore, once the above relationship is established, the detection intensity along the detector array would be constant throughout the entire scanning process, which reflects the dynamic regulation of the proposed Bowtie. Thus, on the basis of $\mu_p = \mu_{water}$, $\mu_w = 0$ and $k = 1/3$ in formula (2), we can get μ_h, which is related to $CeCl_3$ solution concentration. Therefore, we only need to determine the appropriate concentration of $CeCl_3$ solution to ensure that the dynamic range can be compressed.

According to formula (1), if the intensity I is equal to $I_0 \exp(-B_0\mu_h)$, the formula (2) must be established. In Fig.8(a), the intensity detected by the probe point 1 is equal to $I_0 \exp(-B_0\mu_h)$ and that by the probe point 2 is equal to I. So, the formula (2) can be established under the condition that two probes in Fig.8(a) detect the same intensity. As shown in Fig.8(b), the intensities detected by two probe points change with the $CeCl_3$ solution concentration. Two probe points detect the same intensity at 33.36% $CeCl_3$ solution, which is chosen as heavy attenuating liquid filling the HB.

Therefore, the dynamic Bowtie can be designed based on the abovementioned method.

2.3 Data Collection

In simulation, to verify the out-performance of the dynamic Bowtie, we obtained relevant data based on two scan modes of filter: no Bowtie and the dynamic Bowtie. Fig.9 shows 3 scanning geometries for achieving projection data. In the three scanning geometries, the intensity I_0 of source was attenuated to I_p, I_{db} and I_{pdb}, which were obtained by photon flux tallying card. Based on the scanning geometry 1 and the scanning geometry 3, the radiation dose distributions in two scan modes of filter was obtained by radiation dose tallying card.

3 Results

3.1 The Dynamic Range on Detector

Based on the intensity data, the logarithm of the relative detection intensity from circle scans is displayed in Fig.10, where the ray angle γ is obtained according to detector's unit number n

$(0 \le n < 672)$, $\gamma = (335 - n) \times \Delta\gamma$ and the projection angle φ is obtained according to projection number $m\,(0 \le m < 720)$, $\varphi = m \times \Delta\varphi$ $(\Delta\varphi = 2\pi/720)$. For the design phantom, while the dynamic range is large without the Bowtie (Fig.10(a)), the relative detection intensity is almost constant with the dynamic Bowtie (Fig.10(b)). If we define the dynamic range as $\max\left(I\left(n,m\right)\right)/\min\left(I\left(n,m\right)\right)$, the dynamic range is compressed by almost 1293 times under the action of the dynamic Bowtie. Similarly, for the target phantom, the Bowtie can also contribute to the dynamic range. According to the changes seen in Fig.10(c) to Fig.10(d), we can see that the dynamic Bowtie can effectively compress the dynamic range, which is almost compressed by 111 times.

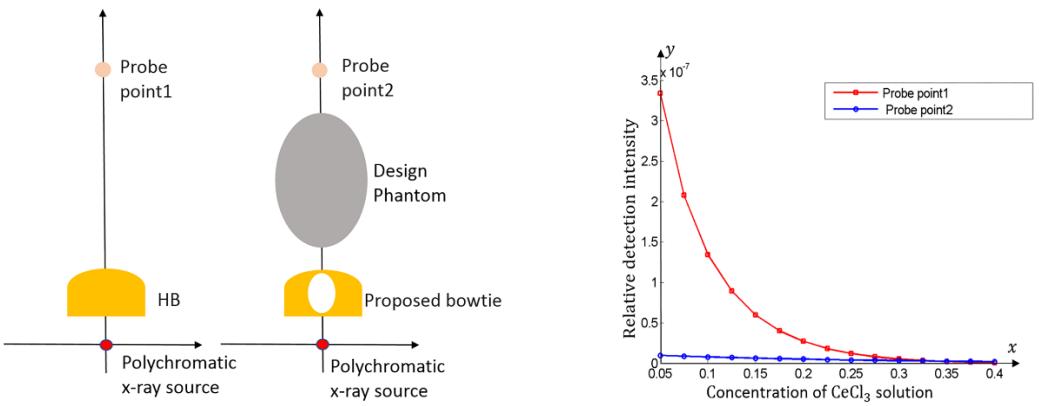

(a) The model determining HB solution concentration (b) The relative detection intensity

Fig.8 Determination of the $CeCl_3$ solution concentration.

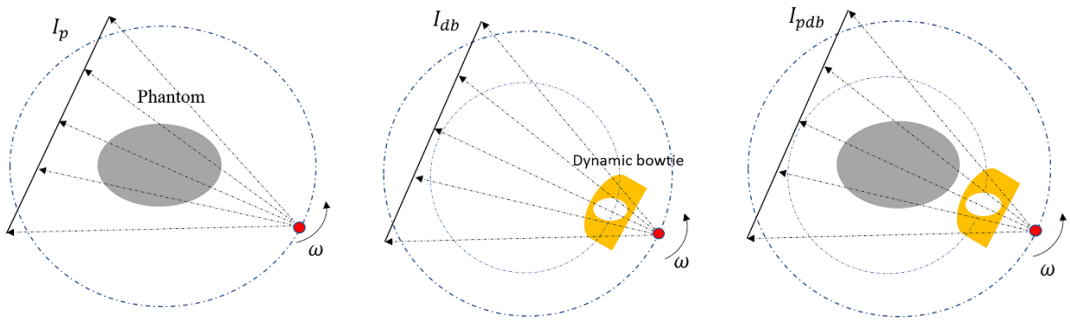

(a) Scanning geometry 1 (b) Scanning geometry 2 (c) Scanning geometry 3

Fig.9 Scanning geometries

3.2 Radiation Dose

The relative dose distributions are shown at projection angles of 0^o, 60^o, 120^o and 240^o in Fig.11. The radiation dose distributions without Bowtie are shown in Fig.11(a) to Fig.11(d) and the radiation dose distributions with the dynamic Bowtie are shown in Fig.11(e) to Fig.11(h). It can be seen from the changes in the first row of figures to the second row of figures that the dynamic Bowtie reduces the radiation exposure away from the central X-ray. Fig.12 shows the total relative dose distributions after summing the dose distributions in all projection angles. Seen from the changes in Fig.12(a) to Fig.12(b), the dynamic Bowtie keeps the object away from severe radiation environment.

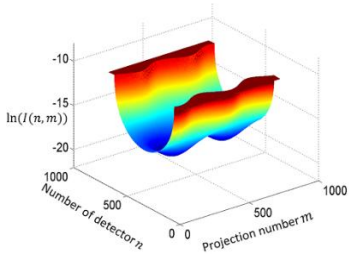

(a) The design phantom for no Bowtie

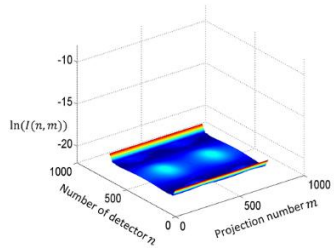

(b) The design phantom for the dynamic Bowtie

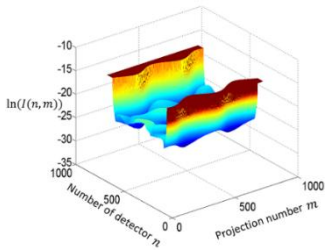

(c) The target phantom for no Bowtie

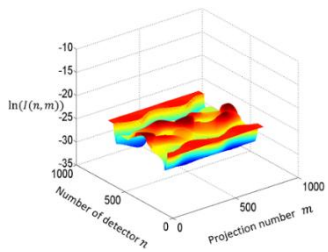

(c) The target phantom for the dynamic Bowtie

Fig.10　Logarithm of relative detection intensity for circle scans.

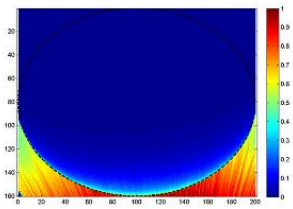

(a) 0^o

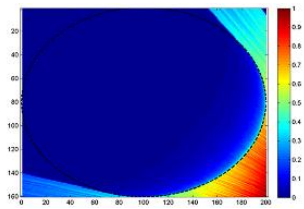

(b) 60^o

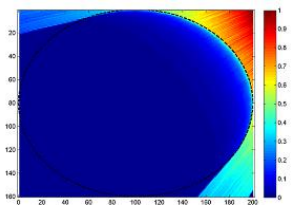

(c) 120^o

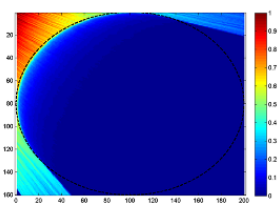

(d) 240^o

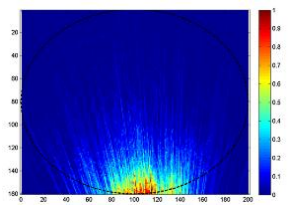

(e) 0^o

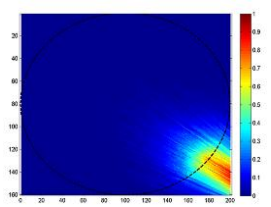

(f) 60^o

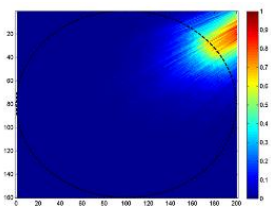

(g) 120^o

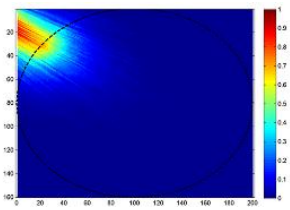

(h) 240^o

Fig.11　The dose distributions for a single projection angle

3.3 Image Quality

According to beer attenuation law, we can obtain the projection of phantoms, which can be expressed as $P_{nb}=\ln\left(I_0/I_p\right)$ for the mode without Bowtie and $P_{db}=\ln\left(I_{db}/I_{pdb}\right)$ for the mode with the dynamic Bowtie. Based on P_{nb} and P_{db}, the reconstructed images of 512×512 pixels are obtained by the filtered back projection (FBP) algorithm.

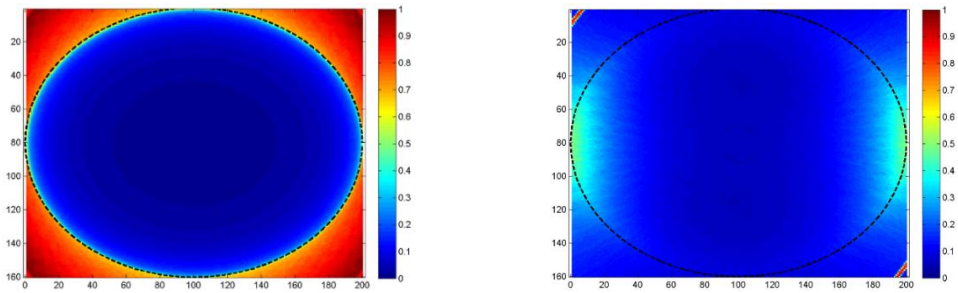

(a) Total distribution for no Bowtie (b) Total distribution for the dynamic Bowtie

Fig.12 The total dose distributions after summing all single dose distribution data

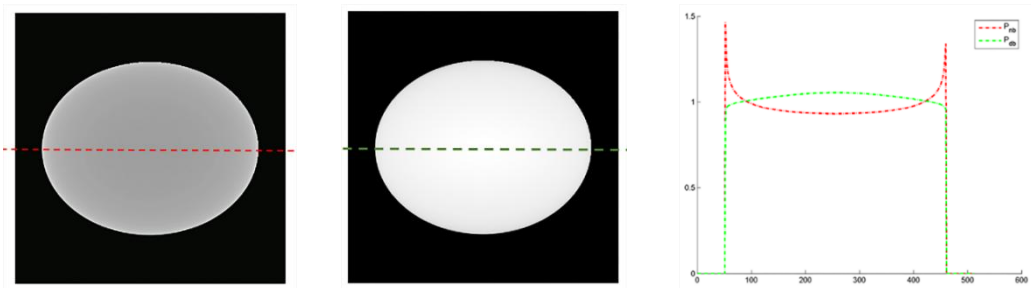

(a) Without Bowtie (b) With the dynamic Bowtie (c) Gray value display

Fig.13 The reconstructed images for the design phantom

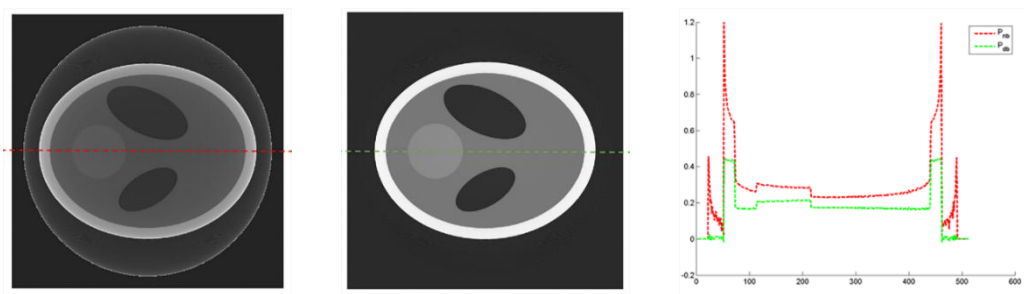

(a) Without Bowtie (b) With the dynamic Bowtie (c) Gray value display

Fig.14 The reconstructed images for the target phantom

For the design phantom, the reconstructed image without Bowtie is shown in Fig.13(a) and the reconstructed image with the dynamic Bowtie is shown in Fig.13(b). The display window is [0, 1.5]. Fig.13(c) shows the gray values on the lines in Fig.13(a) and Fig.13(b). Obviously, the reconstructed image with the dynamic Bowtie is more consistent while the reconstructed image without Bowtie is corroded by serious “cup” artifacts. The standard deviation of reconstructed image is 0.058 for the dynamic Bowtie compared with 0.086 for no Bowtie. The smaller the standard deviation is, the more uniform gray values of reconstructed image are, which more realistically reflects the characteristics of the

design phantom.

The reconstructed images of the target phantom are also shown in Fig.14(a) and Fig.14(b), which are respectively for the mode without Bowtie and the mode with the dynamic Bowtie. The display window is [0, 1.2]. Compared to Fig.14(a), Fig.14(b) is more clear and realistic. The gray values on the lines (Fig.14(c)) indicate that the dynamic Bowtie reduces the noise of the edge of the reconstructed image. The variance of additive zero mean Gaussian noise[22] reduces from 0.079 for no Bowtie to 0.027 for the dynamic Bowtie，which means that the reconstructed image with the has lower noise.

4 Discussion and Conclusions

We have designed the dynamic Bowtie using the abovementioned methodology, which verified that the dynamic Bowtie can contribute benefits in terms of the dynamic range, radiation dose and image quality. In the simulation study, we established simulation frame, which includes model layouts, a target phantom, a reflecting target source and the proposed dynamic Bowtie. Next, we also used a design phantom filled with uniform water to design the dynamic Bowtie and to evaluate its performances. Finally, we acquired the projections from two scanning modes: no Bowtie and the dynamic Bowtie. The results confirmed the outperformance with the dynamic Bowtie in terms of the dynamic range, radiation dose and image quality. A narrow dynamic range means that the dynamic Bowtie contributes a uniform photon flux. As the photon fluxes are uniformed, the benefits in radiation dose and image quality also increase.

The results show that the dynamic Bowtie can reduce the radiation dose irradiated to patients. Compared to no Bowtie, the proposed dynamic Bowtie can reduce the radiation exposure of patients by increasing greater attenuation further from the center region, where X-ray typically pass through less tissue.

The results also show that the dynamic Bowtie can improve the image quality. The results of the design phantom show that hardening artifacts are almost reduced by the dynamic Bowtie. For the target phantom with different attenuation modules, the dynamic Bowtie also shows good performance in image quality. The reasons for the improving image quality are as following. First, similar to a model-based correction method[23], Bowtie filters can reduce beam hardening. As the X-ray do not pierce through the patient, until it is attenuated by the dynamic Bowtie, the X-ray with low energy is filtered. So, the beam-hardening effects are reduced under the action of the dynamic Bowtie. Second, Bowtie filters can reduce the scattering photons[24]. In addition to reducing radiation exposure, scattering photons also reduced. Therefore, the reductions in beam-hardening effects and scattering photons contribute to the improvement of the image quality[25-26].

In recent years, the photon-counting detector has been intensively investigated, as it can be applied to multispectral CT[27-28]. One key challenge is that conventional scan modes have high count rates and photon-counting detectors exhibit count rate loss at high count rates. Especially, the piecewise-linear dynamic Bowtie filter and digital beam attenuator have been debated in conjunction with photon-counting detectors, and results suggest that dynamic Bowtie attenuators can reduce the count rate loss and compress the dynamic range of projections, which indicates that the photon-counting imaging is easier to be implemented with this technique[29]. Therefore, the study of the proposed dynamic Bowtie in conjunction with photon-counting detectors will also be the next focus of our work.

Acknowledgment: This work is primarily supported by the National Natural Science Foundation of China (No. 61471070) and the National Instrumentation Program of China (No. 2013YQ030629). The authors would like to thank the ICT Research Center of Chongqing

University, China, for the support of the simulation study, as well as Dr. Changcheng Gong for valuable discussions and constructive suggestions.

References

[1] Mcnittgray MF. AAPM/RSNA physics tutorial for residents: Topics in CT radiation dose in CT[J]. Radiographics A Review Publication of the Radiological Society of North America Inc, 2002, 22(6): 1541.
[2] Gonz ález ABD, Darby S. The risk of cancer from diagnostic X-rays[J]. Lancet, 2004, 363(9406): 345.
[3] JIANG H. Computed tomography: Principles, design, artifacts, and recent advances[M]. 2ed. Society of Photo-Optical Instrumentation Engineers, 2009.
[4] Hyland M. Quality assurance for computed-tomography simulators and the computed-tomography-simulation process: Report of the AAPM Radiation Therapy Committee Task Group No. 66[J]. Medical Physics, 2003, 30(10): 2762.
[5] Boas FE, Fleischmann D. CT artifacts: Causes and reduction techniques[J]. Imaging in Medicine, 2012, 4(2): 229-240.
[6] Blessing M, Bhagwat MS, Lyatskaya Y, et al. Kilovoltage beam model for flat panel imaging system with bow-tie filter for scatter prediction and correction[J]. Physica Medica, 2012, 28(2): 134-143.
[7] Zhu H, Gao F, Liu F. Review of dynamic Bowtie filter for CT[J]. Chinese Journal of Scientific Instrument, 2017, 38(3): 643-652.
[8] Hsieh S S, Pelc N J. The feasibility of a piecewise-linear dynamic Bowtie filter[J]. Medical Physics, 2013, 40(3): 31910.
[9] Hsieh SS, Pelc NJ. Control algorithms for dynamic attenuators[J]. Medical Physics, 2014, 41(6): 61907.
[10] Szczykutowicz TP, Mistretta CA. Design of a digital beam attenuation system for computed tomography: Part I. System design and simulation framework[J]. Medical Physics, 2013, 40(2): 21905.
[11] Szczykutowicz TP, Mistretta CA. Design of a digital beam attenuation system for computed tomography. Part II. Performance study and initial results[J]. Medical Physics, 2013, 40(2): 21906.
[12] Hsieh SS, Fleischmann D, Pelc NJ. Dose reduction using a dynamic, piecewise-linear attenuator[J]. Medical Physics, 2014, 41(2): 21910.
[13] Liu F, Yang Q, Cong W, et al. Dynamic Bowtie filter for cone-beam/multi-slice CT[J]. Plos One, 2014, 9(7): e103054.
[14] Zhu H, Gao F, Wu W, et al. Dynamic Bowtie filter design with Monte Carlo simulation for cone-beam CT[C]. The Chinese Control and Decision Conference, 2017.
[15] Demarco JJ, Solberg TD, Smathers JB. A CT-based Monte Carlo simulation tool for dosimetry planning and analysis[J]. Medical Physics, 1998, 25(1): 1-11.
[16] Yubai K, Okuhara K, Hirai J. Combining deterministic and Monte Carlo calculations for fast estimation of scatter intensities in CT[J]. Physics in Medicine & Biology, 2006, 51(18): 4567-4586.
[17] Amato E, Italiano A, Leotta S, et al. Monte Carlo study of the dose enhancement effect of gold nanoparticles during X-ray therapies and evaluation of the anti-angiogenic effect on tumour capillary vessels[J]. Journal of X-ray science and technology, 2013, 21(2): 237-247.
[18] Andreo P. Monte Carlo techniques in medical radiation physics[J]. Physics in Medicine & Biology, 1991, 36(7): 861-920.
[19] Xiang L, Samei E, Segars WP, et al. Patient-specific radiation dose and cancer risk estimation in CT: Part I. Development and validation of a Monte Carlo program[J]. Medical Physics, 2011, 38(1): 397.
[20] Team XMC. MCNP - A General Monte Carlo N-Particle Transport Code, Version 5[Z]. 2005: 271, 24922-24926.
[21] Peppler WW, Kudva B, Dobbins JT, et al. Digitally controlled beam attenuator[C]. International Society for Optics and Photonics, 1982:106-111.
[22] Immerkær J. Fast noise variance estimation[J]. Computer Vision & Image Understanding, 1996, 64(2): 300-302.
[23] Casteele EV D, Dyck DV, Sijbers J, et al. A Model-based correction method for beam hardening artefacts in X-ray microtomography[J]. Journal of X-ray Science and Technology, 2004, 12(1): 53-57.
[24] Zhang G, Marshall N, Jacobs R, et al. Bowtie filtration for dedicated cone beam CT of the head and neck: a simulation study[J]. British Journal of Radiology, 2013, 86(1028): 20130002.
[25] Toth TL, Cesmeli E, Ikhlef A. Image quality and dose optimization using novel X-ray source filters

tailored to patient size[J]. Proc Spie, 2005, 5745: 283-291.
[26] Mail N, Moseley DJ, Siewerdsen JH, et al. The influence of Bowtie filtration on cone-beam CT image quality[J]. Medical Physics, 2009, 36(1): 22-32.
[27] Wang X, Meier D, Taguchi K, et al. Material separation in X-ray CT with energy resolved photon-counting detectors[J]. Medical Physics, 2011, 38(3): 1534.
[28] Ballabriga R, Campbell M, Heijne E, et al. Medipix3: A 64 k pixel detector readout chip working in single photon counting mode with improved spectrometric performance[J]. Nuclear Instruments & Methods in Physics Research, 2012, 633(1): S15-S18.
[29] Hsieh SS, Pelc NJ. The piecewise-linear dynamic attenuator reduces the impact of count rate loss with photon-counting detectors[J]. Physics in Medicine & Biology, 2014, 59(11): 2829.

一种锥束 CT 动态 Bowtie 的蒙特卡罗模拟研究

冯绪杨[1]，伍伟文[2]，朱慧杰[2]，余海军[1]，刘丰林[1,2]✉

1. 重庆大学机械工程学院，重庆 400044
2. 重庆大学光电技术及系统教育部重点实验室，重庆 400044

摘要：在 CT 中，前置于患者的衰减器（“Bowtie 滤波器”或“Bowtie”）被用来减少患者所受的辐射剂量和帮助满足探测器的动态范围，同时 Bowtie 也能提高 CT 图像质量。传统的静态滤波器对调制 X 射线能力有限，我们之前提出了一种能够有效调制 X 射线的动态 Bowtie 滤波器。本文使用蒙特卡罗模拟方法设计和研究提议动态 Bowtie 滤波器。首先，建立了一个仿真框架，包括一个目标试样和一个由反射靶生成的多能谱射线源。接着，一个设计试样被用来辅助设计针对于目标试样的动态 Bowtie 滤波器。最后，我们分别从没有 Bowtie 滤波器和带有动态 Bowtie 滤波器两种模式中，模拟获得两个试样的投影数据并进行分析研究。结果显示，在设计的动态 Bowtie 作用下，到达探测器的 X 射线动态范围明显减小、X 射线光子通量一致性很好，并且动态 Bowtie 可以减小辐射剂量和提高 CT 图像质量。

关键词：计算层析成像；锥束；动态 Bowtie；蒙特卡罗仿真

Biography: FENG Xu-yang（1994-），man, he received his bachelor's degree from Chongqing Technology and Business University in 2015. He is currently pursuing a graduate degree in mechanical engineering at Chongqing University, Chongqing, China. His research interests include Mechatronics, Control engineering and CT dynamic Bowtie, Tel: 15730409617，E-mail: fengxy@cqu.edu.cn. LIU Feng-lin✉ (1969-), man, he received a Ph.D. degree from the Mechanical Engineering School, Chongqing University, Chongqing, China, in 2009. He is currently a Professor and the Director of the ICT Research Center, Chongqing University, Chongqing, China. His research interests include X-ray imaging, image reconstruction and industrial CT systems, Tel: 13983075766，E-mail: liufl@cqu.edu.cn.

欢迎订阅《中国体视学与图像分析》

《中国体视学与图像分析》是经国家出版署批准，中国科学技术协会主管、国家一级学会——中国体视学学会主办，全面反映中国体视学理论和图像应用技术研究的学术性和技术性综合刊物。主要报道国内外有关三维结构与图像的定量分析和表征的最新理论与方法，内容涉及体视学、图像分析、三维视觉、三维建模、三维成像与可视化、相关图像的获取（如各种显微镜、CT、物种摄影技术）和处理技术，相关数学原理的研究（如几何概率、分形理论、数学形态学），计算机仿真与信号处理，三维图像技术和定量显微镜技术及其在各专业领域（如生物学、医学、材料科学、地学、矿物学、农学、遥感、计算机、航空等）中的应用。面向广大从事图像技术及体视学研究的高中级科技工作者和高校师生。

本刊为季刊，每季末出版，国内统一刊号：CN 11-3739/R；国际标准刊号 ISSN 1007-1482，国际标准 16 开，是国家科技部中国科技论文统计源期刊(科技核心期刊)、《中国学术期刊综合评价数据库》全文收录期刊、中国期刊网中国学术期刊（光盘版）全文收录期刊、《中国学术期刊文摘》收录期刊、《中国生物医学文献数据库》收录期刊、《中文生物医学期刊文献数据库》收录期刊、《中国生物医学科学引文数据库》收录期刊和《CAJ-CD 规范》执行优秀期刊。

欢迎单位和个人直接向本刊编辑部订阅。每期定价 15 元，全年定价 70 元（含邮寄包装费及邮费）。另外，编辑部尚存有部分过刊出售，欲购者请直接与编辑部联系。

邮局汇款：《中国体视学与图像分析》编辑部
地　　址：北京清华大学工物系刘聊楼 211 室《中国体视学与图像分析》编辑部
邮　　编：100084
电　　话：010-62776336
传　　真：010-62776336
E-mail: tscss@mail.tsinghua.edu.cn
Web: www.tscss.org

银行汇款：
开户行：北京工商银行中关村支行成府路分理处
账　号：0200095709200034877
收款单位：中国体视学学会